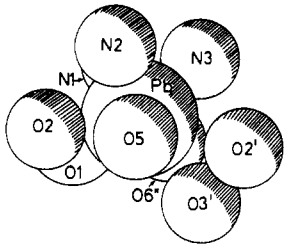

Figure 5. Perspective view of the PbN_3O_6 polyhedron of **2** emphasizing the spatial requirements of the atoms.

length of the nitrate groups of 1.252 Å corresponds to that found in many simple ionic nitrate salts.

The Pb–O distances range from 2.66 to 3.21 Å. There are three short Pb–O bond lengths (2.66, 2.86, 3.05 Å) and three longer ionic interactions at 3.18, 3.21, and 3.21 Å (Figure 4). These values can be compared to the lead–oxygen distances of 2.805 Å in lead nitrate[12] and to those in other N-macrocyclic lead nitrate complexes (2.56–2.87 Å,[14] 2.74–3.17 Å,[3] 2.88–3.31 Å[2]). The sum of the ionic radius of Pb^{2+} and the van der Waals radius of oxygen is 2.67 Å. Therefore, we conclude that the Pb–O bonds in **2** display very little covalency.

The lead centers in **2** attain a coordination number of 6 (three short Pb–N and Pb–O interactions, respectively) or 9 (6 + 3) if the three long Pb–O distances are also taken into consideration. Both polyhedra are quite irregular, but it is interesting to note that the geometries of the PbN_3O_3 polyhedra in **1** and **2** are quite similar (Figure 3b).

This is a clear indication that the lone pair of valence electrons of the LPb^{2+} unit is stereochemically active in the same fashion in compounds **1** and **2**. Figure 5 displays a perspective view of the PbN_3O_6 polyhedron, emphasizing the spatial requirements of the atoms. The lead(II) center is surrounded by three nitrogen atoms, which define a plane above Pb^{2+}; a second nearly parallel plane is then defined by five oxygen atoms below Pb^{2+} (O1, O2, O6″, O2′, O5). It is then clearly seen that the lone pair of electrons of LPb^{2+} points below the latter plane.

Conclusion

We have shown in this work that the small tridentate macrocyclic ligand, 1,4,7-triazacyclononane binds strongly in aqueous solution to lead(II), forming a 1:1 complex with three covalent lead–nitrogen bonds. The LPb^{2+} moiety forms in the solid state three further bonds of highly ionic character to oxygen atoms as in **1** and **2**. The lead(II) centers are then in an environment of six donor atoms forming a highly irregular polyhedron, the shape of which is very similar in both cases. The lone pair of valence electrons of the LPb^{2+} unit appears to be stereochemically active in the same fashion in the two crystal structures under investigation:

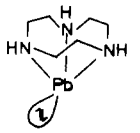

Acknowledgment. Financial support of this work by the Fonds der Chemischen Industrie is gratefully acknowledged.

Registry No. 1, 101630-20-0; 2, 101630-21-1.

Supplementary Material Available: Tables of refined thermal parameters, atomic coordinates of hydrogen atoms, and bond distances and angles for **1** and **2** (5 pages). Ordering information is given on any current masthead page. According to policy instituted Jan 1, 1986, the tables of calculated and observed structure factors (29 pages) are being retained in the editorial office for a period of 1 year following the appearance of this work in print. Inquiries for copies of these materials should be directed to the Editor.

Contribution from the Lehrstuhl für Anorganische Chemie I der Ruhr-Universität, D-4630 Bochum, FRG, Anorganisch-Chemisches Institut der Universität, D-6900 Heidelberg, FRG, and Fachbereich Chemie der Philipps-Universität, D-3550 Marburg/Lahn, FRG

Crystal Structure of Bis[bis(1,4,7-triazacyclononane)nickel(III)] Dithionate Heptahydrate and Its Single-Crystal EPR Spectrum

Karl Wieghardt,*[1a] Wolfgang Walz,[1a] Bernhard Nuber,[1b] Johannes Weiss,[1b] Andrej Ozarowski,[1c] Horst Stratemeier,[1c] and Dirk Reinen*[1c]

Received September 12, 1985

The structure of bis[bis(1,4,7-triazacyclononane)nickel(III)] dithionate heptahydrate, $[Ni(C_6H_{15}N_3)_2]_2(S_2O_6)_3 \cdot 7H_2O$, has been determined. The nickel(III) complex crystallized in the monoclinic system, space group $P2_1/n$, with $a = 8.669$ (7) Å, $b = 28.91$ (2) Å, $c = 9.579$ (7) Å, $\beta = 91.28$ (5)°, and $Z = 2$. The structure was refined to a final R value of 0.061 for 3360 unique reflections. The coordination sphere at the Ni(III) centers consists of six nitrogen atoms of two facially coordinated 1,4,7-triazacyclononane rings in a tetragonally distorted octahedral arrangement. The six nickel–nitrogen bonds form two sets with two longer axial bonds, 2.107 (5) and 2.111 (5) Å, and four shorter equatorial bonds, 1.964 (5), 1.985 (5), 1.970 (5), and 1.965 (5) Å. From the EPR powder and single-crystal spectra an axial **g** tensor ($g_\parallel = 2.03_2$, $g_\perp = 2.12_9$ at 298 K) was deduced. The sequence $g_\perp > g_\parallel \geq g_0$ ($g_0 = 2.00_2$) is compatible only with a $^2A_{1g}$ (d_{z^2}) ground state and a tetragonally elongated NiN_6 octahedron. The first excited high-spin state is estimated to have an energy of about 4000 cm^{-1} with respect to that of the low-spin ground state.

Introduction

Structural information on complexes of nickel in the oxidation state +III are rather scarce. Only a limited number of such complexes have been characterized to date by X-ray determinations due to their generally strong oxidative capabilities. Kinetically stable complexes of Ni(III) containing tetraaza macrocycles and two axially coordinated monodentate ligands have been prepared, and their structures have been determined by X-ray crystallography: *trans*-[dichloro(1,4,8,11-tetraazacyclotetradecane)nickel(III)] perchlorate,[2] $[Ni([14]aneN_4)Cl_2]ClO_4$, and *trans*-[bis(dihydrogen phosphato)(*meso*-5,7,7,12,14,14-hexamethyl-1,4,8,11-tetraazacyclotetradecane)nickel(III)] perchlorate,[3] $[Ni(meso\text{-}Me_6[14]aneN_4)(H_2PO_4)_2]ClO_4$. Recently, the structures of (1,4,7-triazacyclononane-*N*,*N*′,*N*″-triacetato)nickel(III)[4] and of an adduct of tris(2,2′-bipyridine)nickel(III) perchlorate,[5]

(1) (a) Ruhr-Universität Bochum. (b) Universität Heidelberg. (c) Philipps-Universität Marburg.

(2) Ito, T.; Sugimoto, M.; Toriumi, K.; Ito, H. *Chem. Lett.* **1981**, 1477.
(3) Zeigerson, E.; Bar, I.; Bernstein, J.; Kirschenbaum, L. J.; Meyerstein, D. *Inorg. Chem.* **1982**, *21*, 73.
(4) Van der Merwe, M. J.; Boeyens, J. C. A.; Hancock, R. D. *Inorg. Chem.* **1983**, *22*, 3489.
(5) Szalda, D. J.; Macartney, D. H.; Sutin, N. *Inorg. Chem.* **1984**, *23*, 3473.

0020-1669/86/1325-1650$01.50/0

Table I. Experimental Details of the X-ray Diffraction Study of $[NiL_2]_2(S_2O_6)_3 \cdot 7H_2O$

(A) Crystal Parameters at 20 °C			
a, Å	8.669 (7)	mol wt	1240.7
b, Å	28.91 (2)	space group	$P2_1/n$
c, Å	9.579 (7)	ρ(exptl), g cm^{-3}	1.70
β, deg	91.28 (5)	ρ(calcd), g cm^{-3}	1.717
V, Å^3	2400.1	cryst dimens, mm^3	0.04 × 0.3 × 0.3
Z	2		

(B) Measurement of Intensity Data	
instrument	AEDII Siemens
radiation	Mo Kα (λ = 0.710 69 Å), graphite monochromatized
2θ limits, deg	60
scan type	ω
octants collcd	$\pm h,k,l$

(C) Treatment of Intensity Data	
redn to prelim F_o and $\sigma(F_o)$	cor for bkgd, attenuators, and Lorentz–polarization effects of monochromatized X-radiation in usual manner
abs cor	
μ, cm^{-1}	10.7
transmissn coeff: max; min	0.734; 0.474
total no. of reflcns	3414
no. of obsd data with $I > 1.5\sigma(I)$	3360
no. of refined parameters	306

$[Ni(bpy)_3](ClO_4)_3 \cdot 2CH_3CN \cdot 0.5CH_2Cl_2$, have been reported.

Well-characterized complexes of trivalent nickel complexes are of interest in two areas of inorganic chemistry.

(1) ESR spectroscopic evidence seems to indicate that trivalent nickel centers occur in several nickel-containing enzymes,[6] and a number of oligopeptide complexes of nickel(III) have been characterized in solution by Margerum and his co-workers.[7]

(2) In the investigation of electron-transfer barriers and metal–ligand bonding as a function of the metal oxidation state, complexes of nickel(II) and nickel(III) with an identical ligand environment have attracted interest in order to test models for the rate constant k for an electron-exchange reaction[5,8] such as eq 1.

$$M^{II}L^{2+} + M^{III}L^{3+} \overset{k}{\rightleftharpoons} M^{III}L^{3+} + M^{II}L^{2+} \quad (1)$$

We[9] and others[10] have recently reported the preparation of [bis(1,4,7-triazacyclononane)nickel(III)] perchlorate, $[NiL_2](ClO_4)_3$, the first example of a nickel(III) species containing a saturated N_6 donor set that is relatively stable in aqueous solution (pH <7).

We here report an X-ray crystal structure determination of $[NiL_2]_2(S_2O_6)_3 \cdot 7H_2O$ and its single-crystal EPR spectrum. The structure of the corresponding nickel(II) complex has been reported previously.[11]

Experimental Section

$[NiL_2](ClO_4)_3$, where L represents 1,4,7-triazacyclononane ($C_6H_{15}N_3$), has been prepared as described previously.[9] Brown crystals of $[NiL_2]_2(S_2O_6)_3 \cdot 7H_2O$ suitable for single-crystal X-ray determination were grown from an aqueous solution of $[NiL_2](ClO_4)_3$ ($\sim 10^{-3}$ M) at pH 5 (acetic acid) by addition of an aqueous solution of $Na_2S_2O_6 \cdot 2H_2O$ at room temperature in an open vessel.

EPR Investigation. The EPR single-crystal and powder measurements between 298 and 4.2 K were performed with a VARIAN E 15 spectrometer at Q-band frequency.

X-ray Structural Determination of $[NiL_2]_2(S_2O_6)_3 \cdot 7H_2O$. A brown crystal of $[NiL_2]_2(S_2O_6)_3 \cdot 7H_2O$ was attached to the end of a glass fiber and mounted on an AED II Siemens four-circle diffractometer. Preliminary examinations showed that the crystal belonged to the monoclinic system, space group $P2_1/n$ (C_{2h}^5). The unit cell dimensions (22 °C) were obtained by least-squares fit to the setting angles of 30 reflections. The data are summarized in Table I along with details of the treatment of intensity data. An empirical absorption correction was carried out.[12]

Table II. Atomic Coordinates of $[NiL_2]_2(S_2O_6)_3 \cdot 7H_2O$

atom	x	y	z
Ni	0.14972 (9)	0.36057 (3)	0.10182 (9)
S1	0.0487 (2)	0.17967 (6)	0.1510 (2)
S2	0.2604 (2)	0.18018 (6)	0.0401 (2)
S3	0.0317 (2)	0.02045 (6)	0.4132 (2)
N1	0.0147 (5)	0.3123 (2)	0.0222 (5)
N2	0.2316 (5)	0.3663 (2)	−0.1029 (5)
N3	−0.0065 (5)	0.4048 (2)	0.0318 (6)
N4	0.2940 (5)	0.4068 (2)	0.1848 (5)
N5	0.0670 (5)	0.3573 (2)	0.3072 (5)
N6	0.2996 (5)	0.3142 (2)	0.1692 (5)
O1	−0.0294 (5)	0.1385 (2)	0.1041 (6)
O2	−0.0278 (5)	0.2217 (2)	0.1037 (5)
O3	0.0936 (5)	0.1803 (2)	0.2959 (5)
O4	0.3505 (5)	0.1425 (2)	0.1002 (5)
O5	0.3268 (5)	0.2248 (2)	0.0743 (5)
O6	0.2205 (5)	0.1743 (2)	−0.1043 (5)
O31	−0.0530 (6)	0.0004 (2)	0.2965 (5)
O32	−0.0135 (5)	0.0667 (2)	0.4488 (5)
O33	0.1953 (5)	0.0142 (2)	0.4066 (6)
C1	0.0520 (7)	0.3022 (2)	−0.1266 (7)
C2	0.2094 (7)	0.3200 (2)	−0.1615 (7)
C3	0.1440 (7)	0.4029 (2)	−0.1809 (7)
C4	0.0626 (7)	0.4346 (2)	−0.0766 (7)
C5	−0.1489 (7)	0.3791 (2)	−0.0191 (8)
C6	−0.1462 (6)	0.3308 (2)	0.0357 (7)
C7	0.4436 (6)	0.3838 (2)	0.2306 (7)
C8	0.4527 (6)	0.3377 (2)	0.1579 (7)
C9	0.2658 (7)	0.2980 (2)	0.3136 (6)
C10	0.1028 (7)	0.3098 (2)	0.3549 (7)
C11	0.2166 (8)	0.4296 (2)	0.3029 (7)
C12	0.1446 (7)	0.3942 (2)	0.3948 (7)
O_w1	0.3381 (6)	0.0462 (2)	0.7405 (6)
O_w2	0.269 (2)	0.0500 (6)	0.013 (2)
O_w3	0.551 (2)	0.0064 (6)	0.064 (1)
O_w4	−0.014 (2)	0.0454 (7)	0.044 (2)
O_w5	0.304 (2)	0.0477 (7)	0.128 (2)

Table III. Selected Bond Distances (Å) and Angles (deg) for $[NiL_2]_2(S_2O_6)_3 \cdot 7H_2O$

Ni–N1	1.964 (5)	Ni–N4	1.985 (5)
Ni–N2	2.107 (5)	Ni–N5	2.111 (5)
Ni–N3	1.970 (5)	Ni–N6	1.965 (5)
S1–S2	2.141 (3)	S2–O4	1.453 (5)
S1–O1	1.437 (5)	S2–O5	1.446 (5)
S1–O2	1.452 (5)	S2–O6	1.428 (5)
S1–O3	1.434 (5)		
S3–S3′	2.123 (3)		
S3–O23	1.445 (5)		
S3–O32	1.436 (5)		
S3–O33	1.433 (5)		
N1–Ni–N4	176.9 (3)	N1–Ni–N5	96.8 (3)
N1–Ni–N3	86.0 (3)	N4–Ni–N5	83.2 (3)
N4–Ni–N3	97.0 (3)	N5–Ni–N2	177.7 (3)
N2–Ni–N6	97.2 (3)	N2–Ni–N3	82.8 (3)
N1–Ni–N2	84.5 (3)	N1–Ni–N6	91.6 (3)
N4–Ni–N2	95.6 (3)	N4–Ni–N6	85.5 (3)
N5–Ni–N6	84.2 (3)	N5–Ni–N3	95.8 (3)
N6–Ni–N3	177.2 (3)		

(6) (a) Lancaster, J. R. *Science (Washington, D.C.)* **1982**, *216*, 1324. (b) Cammack, R.; Patil, D.; Aguirre, R.; Hatchikian, E. C. *FEBS Lett.* **1982**, *142*, 289. (c) LaGall, J.; Ljundahl, P. O.; Moura, I.; Peck, H. D.; Xavier, A. V.; Moura, J. J.; Teixera, M.; Huynh, B. H.; Der Vartanian, D. V. *Biochem. Biophys. Res. Commun.* **1982**, *106*, 610. (d) Albracht, S. P. J.; Graft, E. G.; Thauer, R. K. *FEBS Lett.* **1982**, *140*, 311. (e) Lancaster, J. R. *FEBS Lett.* **1980**, *115*, 285.
(7) Jacobs, S. A.; Margerum, D. W. *Inorg. Chem.* **1984**, *23*, 1195 and literature therein.
(8) (a) Endicott, J. F.; Kumar, K.; Ramasami, T.; Rotzinger, F. P. *Prog. Inorg. Chem.* **1983**, *30*, 142. (b) Sutin, N. *Prog. Inorg. Chem.* **1983**, *30*, 441. (c) Sutin, N. *Acc. Chem. Res.* **1982**, *15*, 275.
(9) Wieghardt, K.; Schmidt, W.; Herrmann, W.; Küppers, H. J. *Inorg. Chem.* **1983**, *22*, 2953.
(10) McAuley, A.; Norman, P. R.; Olubuyide, O. *Inorg. Chem.* **1984**, *23*, 1939; *J. Chem. Soc., Dalton Trans.* **1984**, *1501*.
(11) Zompa, L. J.; Margulis, T. N. *Inorg. Chim. Acta* **1978**, *28*, L157.

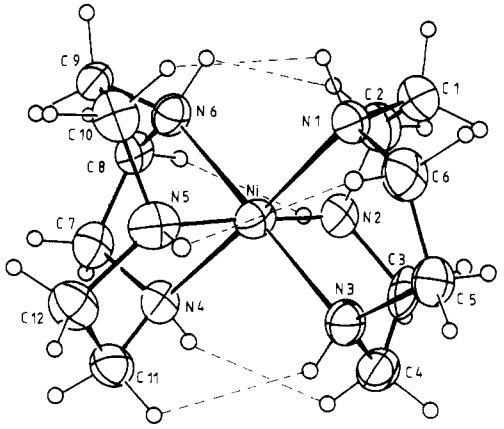

Figure 1. Perspective view and atomic labeling of the cation $[NiL_2]^{3+}$ showing the interligand H–H nonbonded repulsions (---).

The structure was solved via three-dimensional Patterson and Fourier syntheses. Idealized positions of the methylene and amine H atoms were calculated and included in the refinement cycles with a common isotropic thermal parameter (U = 0.045 (5) Å^2). The positions of the oxygen atoms of the molecules of water of crystallization were difficult to locate due to their high mobility in the crystal at room temperature, which is indicated by large isotropic temperature factors of these oxygen atoms and a disordered distribution within the unit cell. O_w^2 and O_w^5 have a separation of only 1.14 Å, and the distance O_w^3–$O_w^{3'}$ is 1.54 Å. Refinements were carried out with an occupancy factor of 0.5 for O_w^2, O_w^5, and O_w^3, respectively. The H atoms of the disordered H_2O molecules were not located. The function minimized during least-squares refinements was $\sum w(|F_o| - |F_c|)^2$ with final convergence to $R = \sum||F_o| - |F_c||/\sum|F_o| = 0.061$ and $R_w = [\sum w(||F_o| - |F_c||)^2/\sum w|F_o|^2]^{1/2} = 0.050$ ($w = 1/\sigma^2(F)$). Scattering factors for all atoms were taken from ref 13. The real and imaginary parts of anomalous dispersion for all non-hydrogen atoms were included. The final atomic parameters are given in Table II and selected bond distances and angles in Table III. Listings of anisotropic thermal parameters, coordinates of H-atoms, and C-C and C-N bond distances are available as supplementary material.

Results and Discussion

Description of the Structure. A view of the $[Ni(C_6H_{15}N_3)_2]^{3+}$ ion and the atom-labeling scheme used are shown in Figure 1. The six saturated, secondary amine nitrogen atoms of the two facially coordinated 1,4,7-triazacyclononane ligands form a tetragonally distorted octahedron about the Ni^{3+} center. The six Ni–N bonds form two sets so that two of the six Ni–N bonds are 2.110 (5) Å and four are 1.971 (5) Å. The four shorter bonds form an equatorial plane while the two longer bonds are in the axial positions. The Ni(III) complex thus exhibits a Jahn–Teller distortion, with the axial bonds 0.139 Å longer than the equatorial bonds (tetragonally elongated octahedron). The Jahn–Teller distortion is expected for a low-spin Ni^{3+} ion in an octahedral environment ($t_{2g}^6e_g^1$). The effective magnetic moment of 2.0 μ_B at 20 °C measured for $[NiL_2](ClO_4)_3$ is in agreement with a low-spin d^7 electronic configuration. In $[NiL_2](NO_3)Cl\cdot H_2O$, which contains nickel(II) centers in a nearly regular octahedral environment of two 1,4,7-triazacyclononane ligands, an average Ni–N bond distance of 2.10 Å has been reported.[11] The axial Ni–N bonds of $[NiL_2]^{3+}$ are 0.01 Å longer whereas the equatorial bonds are shorter by 0.129 Å than in the corresponding Ni(II) complex.

The bond lengths and angles within the 1,4,7-triazacyclononane ligands (average N–C and C–C bond lengths of 1.494 (8) and 1.508 (8) Å, respectively) are similar to those found in other structures and show no unusual features.

There are four cations and six dithionate anions in the unit cell. The sulfur and oxygen atoms of four $S_2O_6^{2-}$ anions occupy symmetry-unrelated positions, respectively. Two further $S_2O_6^{2-}$ anions are on a crystallographic inversion center. In both cases the SO_3^- halves of an $S_2O_6^{2-}$ anion show the usual staggered configuration. Average S–O and S–S bond lengths are 1.442 (5) and 2.132 (3) Å, respectively. Molecules of water of crystallization are distributed in large cavities generated by the approximately spherical shape of the cations and the rather large and nonspherical dithionate anions. Their exact positions have not been precisely located due to a relatively high mobility within the crystal at room temperature. An exception is the oxygen atom O_w1 of one of the water molecules of crystallization, which is strongly hydrogen-bonded to N3 of the cyclic amine and O31′ of a dithionate anion (N3···O_w1 = 2.818 (8) Å and O_w1···O31′ = 2.830 (7) Å).

Comparison with Other Structures. The structure of $[Ni(bpy)_3](ClO_4)_3\cdot 2CH_3CN\cdot 0.5\ CH_2Cl_2$ represents the only other example for a low-spin Ni^{3+} ion in an octahedral environment of six nitrogen atoms. Sutin et al. have determined the crystal structure of this compound at 160 K and have found that the six nickel–nitrogen bonds form three sets with two pairs of longer equatorial bonds (2.022 (6) and 2.000 (5) Å) and a pair of shorter axial bonds (1.924 (6) Å). From these data the authors have concluded that the single unpaired electron of Ni(III) is in the $d_{x^2-y^2}$ rather than in the d_{z^2} orbital. This interpretation is discussed further below.

It is of interest to compare the short Ni–N bonds in $[Ni(bpy)_3]^{3+}$ (1.924 (6) Å) and in Ni(TCTA) (1.93 (1) Å)[4] with the significantly longer average Ni–N distance of the four shorter equatorial Ni–N bonds in $[NiL_2]^{3+}$ (1.971 (5) Å).

We propose that this results from nonbonded repulsions between the two cyclic amine ligands in $[NiL_2]^{3+}$, which are effected by interligand H–H nonbonded repulsions and intraligand repulsions, as depicted in Figure 1. Hancock et al. have recently shown, using empirical force-field calculations, that the ideal, strain-free M–N bond length in $[ML_2]^{2+}$ complexes is 2.09 Å, which is very close to the value found in $[NiL_2]^{2+}$.[14]

In other words, the cavity generated by two 1,4,7-triazacyclononane ligands is too large for the smaller nickel(III). The same effect has been noted for $[CoL_2]^{3+}$, where a Co–N bond length of 1.97 Å has been observed whereas a much shorter distance of 1.92 Å has been calculated for a strain-free Co–N bond distance. In addition, in the low-spin complexes of $[FeL_2]^{2+/3+}$, Fe–N bonds of 2.03 and 1.99 Å have been observed whereas strain-free Fe–N lengths of 1.94 Å for Fe(III) and 1.96 Å for Fe(II) have been calculated.[15]

Spectroscopic Properties of $[NiL_2]^{3+}$. Ni^{3+} in octahedral coordination is low-spin configurated even in cases of rather weak ligands.[16,17] As for Cu^{2+} the ^2E_g ground state is strongly σ-antibonding and subject to a strong Jahn–Teller interaction with the octahedral ϵ-vibration, which usually leads to a very distinct tetragonal elongation. A radial distortion parameter ρ (=16 pm) is derived for the $[NiL_2]^{3+}$ polyhedron from the structural data, which matches quite well with the reported value ($\rho \simeq 14$ pm) for Cs_2KNiF_6.[16] ρ is defined as $(2(\Delta i)^2)^{1/2}$, where the Δi (i = x, y, z) are the deviations of the Ni^{3+}–ligand spacings from the average bond length. The ground state splitting, which is equivalent to the broad low-energy band in the ligand field reflection spectra, is about 6500 cm^{-1} for F$^-$[17] and the triazacyclonane ligand as well. Further bands below 30 000 cm^{-1} are found at 18 000 and 24 000 cm^{-1} together with a shoulder at $\simeq$28 500 cm^{-1}, which may be tentatively assigned to the transitions from the $^2A_{1g}$ ground state to the split levels of the excited octahedral parent states $^2_aT_{1g}$, $^2_aT_{2g}$, and $^2_bT_{1g}$.[17] The g values taken from the EPR powder spectrum (Figure 2) at 298 K (150 K) are axial, with $g_\parallel = 2.03_1$ (2.02_6) and $g_\perp = 2.12_9$ (2.12_8). The sequence $g_\perp > g_\parallel \geq g_0$ [$g_0 = 2.00_2$] is compatible only with a $^2A_{1g}$ (d_{z^2})

(12) Computations were carried out on a Nova (General Data) computer using the SHELXTL program package (revision 3.0, July 1981) by G. M. Sheldrick, Universität Göttingen.
(13) *International Tables for X-ray Crystallography*; Kynoch: Birmingham, England, 1974; Vol. 4.
(14) Thöm, V. J.; Boeyens, J. C. A.; McDougall, G. J.; Hancock, R. D. *J. Am. Chem. Soc.* **1984**, *106*, 3198.
(15) Boeyens, J. C. A.; Forbes, A.; Hancock, R. D.; Wieghardt, K. *Inorg. Chem.* **1985**, *24*, 2926.
(16) Reinen, D.; Friebel, C. *Struct. Bonding (Berlin)* **1979**, *37*, 1.
(17) Reinen, D.; Friebel, C.; Propach, V. *Z. Anorg. Allg. Chem.* **1974**, *408*, 187.

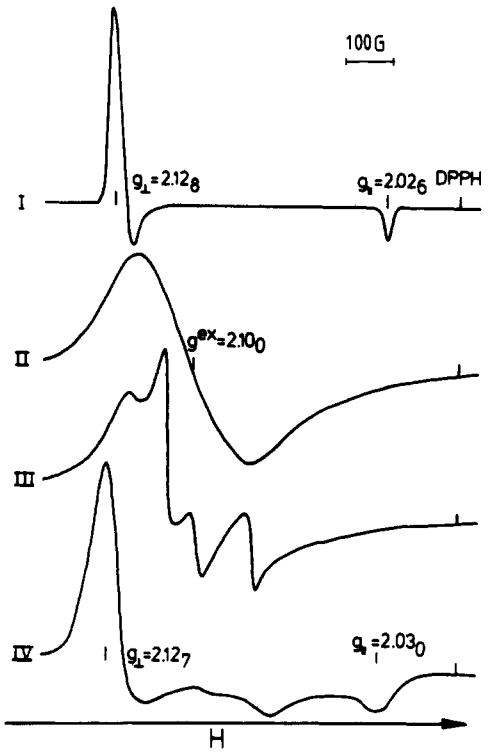

Figure 2. EPR powder spectra (35 GHz) of $[NiL_2]_3(S_2O_6)_3$ at 150 K (I) and of $[NiL_2](ClO_4)_3$ at 298 K (II) and 4.2 K (III). IV is the frozen-DMF-solution (150 K) spectrum of $[NiL_2](ClO_4)_3$ (the signal between $g_\parallel$ and $g_\perp$ corresponding apparently to the dynamically averaged g value).

ground state and hence a tetragonally *enlongated* octahedron. A $^2B_{1g}$ ($d_{x^2-y^2}$) ground state and a compressed octadedron would imply **g**-tensor components of magnitudes $g_\parallel > g_\perp > g_0$. Explicitly, one obtains the following perturbation expression for the g values of an elongated octahedron:[18]

$$g_\parallel = g_0 + 2\frac{\zeta^2}{\delta^2} \equiv g_0 + 2\mu'$$

$$g_\perp = g_0 + 3\zeta\left[\frac{1.38}{E_3} + \frac{0.62}{E_4}\right] + 2\frac{\zeta^2}{\delta^2} \equiv g_0 + 6\mu + 2\mu' \qquad (2)$$

ζ is the effective spin–orbit coupling parameter; δ is the energy separation between the low-spin ground state ($^2A_{1g}$) and the first excited high-spin state (split level of the octahedral $^4T_{1g}$ parent state); E_3 and E_4 are the transitions from $^2A_{1g}$ to the octahedral $^2_aT_{2g}$ and $^2_bT_{2g}$ parent states. With the energy values $\zeta = 450$ cm^{-1}, $E_3 \simeq 24\,000$ cm^{-1}, and $E_4 \simeq 34\,000$ cm^{-1}, which are estimated from the ligand field spectrum and in comparison to F^- as a ligand,[17] one can reproduce the experimental g values rather well, if a high-spin–low-spin separation of about 4000 cm^{-1} is chosen.

The unit cell of $[NiL_2]_2(S_2O_6)_3$ contains four $[NiL_2]^{3+}$ polyhedra, from which only two are magnetically inequivalent. The shortest distance between such a pair is 9.1 Å. Hence, two signals should be observed in the single-crystal EPR experiment, if exchange narrowing does not occur. The orientations of the long axes of the two inequivalent NiN_6 polyhedra are very similar; however, they are included by less than ±4° with respect to the *ac* plane. Accordingly, two signals are resolved only at certain orientations and only in the *ab* plane, even in the 35-GHz experiment. The **g**-tensor components deduced from the angular dependence, which is shown in Figure 3 for one polyhedron, are $g_\parallel = 2.03_4$ and $g_\perp = 2.12_8$ at 35 GHz and 298 K—consistent with the power values. $g_\perp$ is not split within an error limit of 0.00_4 and is located in the plane of nitrogen atoms 1, 3, 4, and 6 (Figure 1). $g_\parallel$ is correlated with the normal to this plane, which deviates

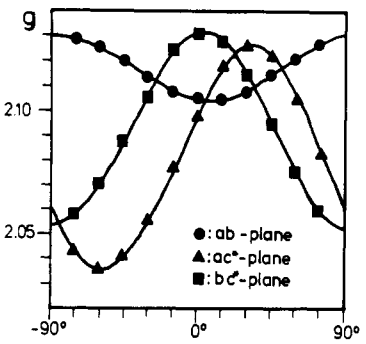

Figure 3. Angular dependence of the **g** tensor of one NiN_6 polyhedron in $[NiL_2]_2(S_2O_6)_3$ in the *ac**, *ab*, and *bc** planes of the monoclinic unit cell (35 GHz, 298 K). The angles −90, 0° correspond to the *b*, *a*,*c**,*a*, and *c**,*b* directions in the *ab*, *ac**, and *bc** planes, respectively.

from the directions of the long Ni–N distances by about 9°. The single-crystal experiment confirms that the unpaired electron is in the d_{z^2} orbital, and hence the NiN_6 octahedron is tetragonally elongated. The EPR powder (Figure 2, part I) and single-crystal signals ($\Delta H_{pp} \simeq 30 \pm 10$ G) are rather narrow. Because the $Ni^{III}N_6$ polyhedra are not sufficiently isolated in the unit cell, the nitrogen hyperfine structure is obviously averaged by exchange narrowing. A frozen-solution spectrum could not be taken because the $S_2O_6^{2-}$ salt is either insoluble or unstable in solvents.

We have also collected spectroscopic data for the complex $[NiL_2](ClO_4)_3$, the structure of which is not known. While the ligand field spectrum is practically identical with the one of the compound with the $S_2O_6^{2-}$ counterion, the EPR spectrum is clearly indicative of exchange narrowing (Figure 2). At 4.2 K a well-resolved structure is observed, which may be due to zero-field splitting effects induced by exchange coupling between the NiL_2^{3+} polyhedra. At 298 K only a broad asymmetric signal appears, which is possibly caused by the onset of a dynamical averaging process in the Jahn–Teller-distorted NiN_6 octahedra. We have made no attempts to assign the spectra and to elucidate the relevant parameters because of the lack of suitable single crystals. The complex is easily dissolved as a stable species in DMF. The frozen-solution spectrum (35 GHz, 150 K) proves that the underlying molecular **g** tensor is equivalent to the one measured for $[NiL_2]_2(S_2O_6)_3$ (Figure 2). Thus a d_{z^2} ground state and a tetragonal elongation of the NiN_6 octahedra of the same extent as for the dithionate complex (at least at lower temperatures) are found in this case also, if one takes the result of identical ligand field reflection spectra additionally into account. The frozen-solution spectrum of the perchlorate salt (Figure 2, part IV) is much broader than the one of solid $[NiL_2]_2(S_2O_6)_3$ (Figure 2, part I), presumably because of the presence of nitrogen hyperfine coupling. The corresponding structure could not be resolved in both the $g_\parallel$ and $g_\perp$ signal, however, even in very diluted DMF solutions. An estimated upper limit for $A_\parallel$ is 20 G.

The g values derived for $[NiL_2]^{3+}$ are also very similar to those reported for $[Ni(bpy)_3]^{3+}$ in frozen solution at 77 K ($g_\parallel = 2.02_7$, $g_\perp = 2.13_7$; 9.5 GHz).[19] The latter spectrum gives even additional evidence for a d_{z^2} ground state, because the observed nitrogen hyperfine structure reflects only the two axial ligands along the molecular z direction. It is interesting in this connection that *compressed* Ni(III) octahedra have been found in the 160 K structure of $[Ni(bpy)_3](ClO_4)_3 \cdot 2CH_3CN \cdot 0.5CH_2Cl_2$, with two short axial Ni–N bond lengths of 1.92_5 Å, and perpendicular to them, four long spacings of 2.01_5 Å.[5] This finding does not match with the frozen-solution EPR spectrum.[19] The different behavior of the EPR spectrum for the solid compound with respect to the one taken in the glassy medium could be explained if a static or dynamic disorder in the equatorial bonds would be present. This effect would split the set of four long spacings (2.01 Å) into two pairs with bond lengths of 1.92_5 and 2.09_5 Å, respectively, in the extreme case. In this way an elongated coordination would result,

(18) Lacroix, R.; Hoechli, V; Müller, K. A. *Helv. Phys. Acta* **1964**, *37*, 627.

(19) Brodovitch, J. C.; Haines, R. I.; McAuley, A. *Can. J. Chem.* **1981**, *59*, 1610.

with a radial distortion parameter ($\rho \simeq 19$ pm) that is only slightly larger than the one for $[NiL_2]^{3+}$. Such a phenomenon of a "planar dynamics" of an "antiferrodistortive order of elongated octahedra" (static, cooperative case) is well-known in the stereochemistry of d^9, d^4, and low-spin d^7 cations with E_g ground states, in particular for Cu^{2+}.[16] This sort of dynamic or nonresolved antiferrodistortive order should result in thermal ellipsoids of four nitrogen ligator atoms that are strongly elongated along the corresponding Ni–N bonds, however, as observed for the $[Cu(NO_2)_6]^{4-}$ entity in the β'-modification of $Cs_2PbCu(NO_2)_6$, for example.[20] Analogous efects are not found for $[Ni(bpy)_3](ClO_4)_3 \cdot 2CH_3CN \cdot 0.5CH_2Cl_2$. Presumably, the static compression in the solid state is stabilized by energetically efficient steric ligand or packing effects. As is well-known from the potential energy surface, which results from the vibronic coupling of an electronic E ground state with the vibrational ϵ-mode, the energy difference between an elongated and compressed D_{4h} geometry is not very large.[16] EPR spectroscopy, in particular on single crystals, would be the probe technique of choice for a final experimental decision. The **g** tensor of a compressed octahedron ($d_{x^2-y^2}$ ground state)[18]

$$g_\parallel' = g_0 + 8\mu + 2\mu' \qquad g_\perp' = g_0 + 2\mu + 2\mu' \tag{3}$$

(see the short-hand notations in eq 1 has the sequence of g values $g_\parallel' > g_\perp' > g_0$, in contrast to $g_\perp > g_\parallel \geq g_0$ for the elongated octahedron (eq 1). In case of a "planar dynamics" or an antiferrodistortive order of elongated octahedra with exchange-coupled **g** tensors, the following averaged g values are expected:

$$\bar{g}_\parallel = g_\perp = g_0 + 6\mu + 2\mu'$$
$$\bar{g}_\perp = \tfrac{1}{2}(g_\parallel + g_\perp) = g_0 + 3\mu + 2\mu' \tag{4}$$

Though the sequence $\bar{g}_\parallel > \bar{g}_\perp \; g_0$ is the same as for a $d_{x^2-y^2}$ ground state, the orbital contribution μ to the g values are rather different in the two cases (eq 2 and 3). Because the contribution μ', resulting from the singlet–triplet separation, is rather small in case of nitrogen as the ligator atom (see above), it should be possible to distinguish between the cases represented by eq 2 and 3 by carefully checking the deviations of the g values for g_0. For Cu^{2+} this can indeed easily be done.[16] Finally, it should be mentioned that for Co^{2+} in octahedral coordination, which is also low-spin in the presence of strong ligands, a d_{z^2} ground state and an elongated coordination are well established,[21] in correspondence to the case of Ni^{3+}.

Acknowledgment. Financial support of this work by the Deutsche Forschungsgemeinschaft and the Fonds der Chemischen Industrie is gratefully acknowledged.

Registry No. $[NiL_2](ClO_4)_3$, 86709-82-2; $[NiL_2]_2(S_2O_6)_3 \cdot 7H_2O$, 101630-19-7.

Supplementary Material Available: Listings of thermal parameters, positional parameters of hydrogen atoms, and C–C and C–N bond lengths (4 pages). Ordering information is given on any current masthead page. According to policy instituted Jan 1, 1986, the tables of calculated and observed structure factors (17 pages) are being retained in the editorial office for a period of 1 year following the appearance of this work in print. Inquiries for copies of these materials should be directed to the Editor.

(20) Mullen, D.; Heger, G.; Reinen, D. *Solid State Commun.* **1975**, *17*, 1249.

(21) Kremer, S.; Henke, W.; Reinen, D. *Inorg. Chem.* **1982**, *21*, 3013.

Contribution from the Lehrstuhl für Anorganische Chemie I der Ruhr-Universität, D-4630 Bochum, FRG, and Anorganisch-Chemisches Institut der Universität, D-6900 Heidelberg, FRG

Macrocyclic Complexes of Indium(III): Novel μ-Hydroxo- and μ-Oxo-Bridged Complexes. Crystal Structures of $[L_4In_4(\mu\text{-}OH)_6](S_2O_6)_3 \cdot 4H_2O$ and $[L_2In_2(CH_3CO_2)_4(\mu\text{-}O)] \cdot 2NaClO_4$ (L = 1,4,7-Triazacyclononane)

Karl Wieghardt,*[1a] Michael Kleine-Boymann,[1a] Bernhard Nuber,[1b] and Johannes Weiss[1b]

Received October 18, 1985

Indium(III) chloride reacted with the macrocyclic ligands (1:1) 1,4,7-triazacyclononane (L), 1,4,7-trimethyl-1,4,7-triazacyclononane (L'), and 1,4,7-trithiacyclononane (L'') in chloroform (acetonitrile) to yield at 60 °C the complexes $LInCl_3$, $L'InCl_3$, and $L''InCl_3$, respectively. $LInBr_3$ was prepared analogously in aqueous solution. Hydrolysis of $LInBr_3$ in alkaline aqueous solution afforded the colorless, tetrameric cation $[L_4In_4(\mu\text{-}OH)_6]^{6+}$, the first well-characterized μ-hydroxo complex of indium(III), which has been isolated as the perchlorate, dithionate, iodide, and hexafluorophosphate salts, respectively. $[L_4In_4(\mu\text{-}OH)_6](S_2O_6)_3 \cdot 4H_2O$ crystallizes in the orthorhombic space group $P2_12_12_1$ with $a = 14.56$ (1) Å, $b = 16.38$ (1) Å, $c = 25.09$ (2) Å, $V = 5983.8$ Å^3, and $d_{calcd} = 1.810$ g cm^{-3} for $Z = 4$ and molecular weight 1630.6. Least-squares refinement of the structure based on 4293 observations led to a final discrepancy index of $R = 0.074$. The structure consists of discrete tetrameric cations and dithionate anions. The $In_4(OH)_6$ core has an adamantane-like skeleton. The average In–O bond distance is 2.14 (1) Å. Hydrolysis of $LInBr_3$ in 2 M sodium acetate at 60 °C and addition of sodium perchlorate yielded colorless crystals of $[L_2In_2(CH_3CO_2)_4(\mu\text{-}O)] \cdot 2NaClO_4$, which crystallizes in the triclinic space group $P\bar{1}$ with $a = 11.445$ (6) Å, $b = 11.846$ (7) Å, $c = 14.986$ (9) Å, $\alpha = 76.22$ (5)°, $\beta = 67.94$ (5)°, $\gamma = 67.53$ (4)°, $V = 1729.4$ Å^3, and $d_{calcd} = 1.85$ g cm^{-3} for $Z = 2$ and molecular weight 985.1. Least-squares refinement of the structure based on 7713 reflections led to a final R value of 0.057. The structure consists of the neutral, μ-oxo-bridged dimer $[L_2In_2(CH_3CO_2)_4(\mu\text{-}O)]$ and sodium perchlorate. The average In–O bond distance of the oxo bridge is 2.114 (4) Å.

Introduction

Recently, the hydrolysis of indium(III) in aqueous solution has been investigated by potentiometric titration at 25 °C in 0.1 M potassium nitrate.[2] The occurrence of the monomeric hydroxo species $InOH^{2+}$ and $In(OH)_2^+$ has been confirmed in this study, but species of higher nuclearity have also been proposed such as $In_p(OH)_p^{2p+}$. The best fit for a model with $p = 4$ has been obtained; e.g., a tetrameric μ-hydroxo-bridged species has been suggested to exist in aqueous solution at higher pH. A search of the literature revealed that—surprisingly enough—no well-defined μ-hydroxo-bridged complexes of indium(III) have been synthesized and characterized by X-ray crystallography.

We have in the past few years used a simple synthetic route to μ-hydroxo-bridged complexes of transition metals, which used monomeric complexes of the type LMX_3 (L represents small, tridentate macrocyclic, N-donor ligands and X^- is a monodentate ligand (Cl^-, Br^-)) as starting materials that undergo hydrolysis reactions in alkaline aqueous solution. Due to the inherent thermodynamic and kinetic stability of the LM moiety, in many cases no dissociation of the ligands L occurred and formation of various μ-hydroxo- and/or μ-oxo-bridged complexes (dimeric,[3]

(1) (a) Ruhr-Universität Bochum. (b) Universität Heidelberg.
(2) Brown, P. L.; Ellis, J.; Sylva, R. N. *J. Chem. Soc., Dalton Trans.* **1982**, 1911.

0020-1669/86/1325-1654$01.50/0